Title

Adsorption and Decomposition of a Lignin β-O-4 Linkage Model, 2-Phenoxyethanol, on Pt(111): Combination of Experiments and First-Principles Calculations

Journal

The Journal of Physical Chemistry C, 121(18)

ISSN

1932-7447

Authors

Hamou, Cherif A Ould
Réocreux, Romain
Sautet, Philippe
et al.

Publication Date

2017-05-11

DOI

10.1021/acs.jpcc.7b01099

Peer reviewed

Adsorption and Decomposition of a Lignin β-O-4 Linkage Model, 2-phenoxyethanol, on Pt(111): Combination of Experiments and First Principles Calculations

Cherif A. Ould Hamou,[†,§] Romain Réocreux,[‡] Philippe Sautet,[‡,&] Carine Michel,[‡,*] Javier B. Giorgi,[†,‖,*]

[†] Centre for Catalysis Research and Innovation, [§] Department of Physics, [‖] Department of Chemistry and Biomolecular Sciences, University of Ottawa, 10 Marie Curie Pvt., Ottawa, Ontario, Canada. K1N 6N5.

[‡] Univ Lyon, Ens de Lyon, CNRS UMR 5182, Université Claude Bernard Lyon 1, Laboratoire de Chimie, F-69342, Lyon, France

[&] Department of Chemical and Biomolecular engineering, University of California, Los Angeles, Los Angeles, CA 90095, United States

Abstract

To sustain the current attempts in valorizing lignin-based derivatives, this study focuses on the decomposition upon a temperature ramp of 2-phenoxyethanol, a model for the β-O-4 linkage in lignin, on a Pt(111) surface. Under ultra-high vacuum conditions, benzene, hydrogen and carbon monoxide are the main desorbing products. Although benzene is the only aromatic desorbed product at low initial molecular coverages, very small amounts of phenol can be detected at higher initial coverage. Combining X-ray photoelectron spectroscopy and temperature programmed desorption experiments together with density functional theory calculations, a reaction mechanism is suggested, starting with the OH bond scission. Phenoxy PhO is proposed as a key surface intermediate that preferentially deoxygenates rather than desorbs as phenol, similarly to the case of anisole. This behavior, typical of ultra-high vacuum conditions, is attributed to the reducing properties of carbonaceous surface species that efficiently deoxygenate phenoxy and afford the formation of the very stable carbon monoxide.

Key-words: 2-phenoxyethanol, mechanism, decomposition, TPD, DFT, XPS, lignin

Introduction

Biomass is a sustainable and renewable feedstock for potentially high value chemicals that, due to its abundance, could theoretically supply the world demand.[1] Alternatively it could produce up to 10%-14% of the world's energy usage.[2] Lignin, an important biomass component, is the second most abundant polymer in wood and represents up to 40% of the dry biomass weight. While the lignin specific formulation is variable,[3–5] each of its monomers consists of one aromatic oxygenate unit. The removal of oxygen to produce higher value compounds is a necessity but it still remains one of the challenging tasks for lignin exploitation (via pyrolysis, hydrolysis, oxidation, etc).[6,7] Pyrolysis is the most studied method for conversion of lignin and removal of oxygen linkages. It is an effective method to liquefy lignin in order to produce bio-oils.[8,9] However, the separation of the products can be challenging and costly. In contrast, heterogeneous catalysis seems to be the key solution for the conversion of lignin, as the products and the catalyst can be easily separated. Regardless, since thermal decomposition leads to a variable and often uncontrolled product range of the target products, catalysis plays an essential role in making biomass conversion viable for valorization by reducing activation energies for reaction and guiding product selectivity. 2-phenoxyethanol (2-PE), with its aryl and alkyl ether function, is used here as a model of the quintessential β-O-4 linkage, one of lignin's dominant structural motifs which provides more than half of the linkage structures. In this study that combines surface science and modeling, its reactivity is investigated on the platinum Pt(111) model surface as a model catalyst in order to compare the facility of the C-H vs. C-O vs. C-C bonds cleavage (Figure 1).

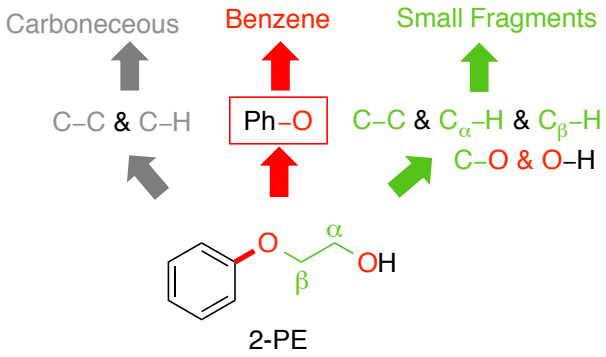

***Figure 1**: Potential decomposition pathways 2-phenoxyethanol (2-PE): in grey, the fragmentation of the aromatic ring; in red the targeted Ph-O cleavage; in green, the decomposition of the ethanol arm.*

As a substituted aromatic compound, 2-PE can undergo a decomposition scheme that is, in principle, related to simpler aromatics like phenol, anisole, etc. Single crystal investigations of aromatic oxygenates on transition metal surfaces have shown different preferences in C-H, C-O and C-C bond cleavage.[10–13] The decomposition pathways of aromatics are strongly dependent

on the coverage of adsorbed molecules on the surface and the interaction strength of the aromatic ring with the catalyst.[10–13]

In the study of the binding of lignin model molecules such as 2-PE to a metal surface, the importance of the aromatic ring is affected by the binding of the phenyl group to oxygen. Molecules with this phenoxy moiety could be expected to behave differently from non oxygenated-aromatics. As such, previous studies of phenol-catalyst interactions are relevant. Phenol has been widely studied on different noble metals. On Pt(111), phenol in a multilayer desorbs from the surface at 195 K while in the second layer at 225 K.[11] Between 0.7 to 1 ML, the O-H bond cleavage occurs below 200 K and phenoxy is subject to a competitive reaction pathway. It either generates benzene and surface oxygen, or it decomposes into CO, H_2 and hydrocarbons. Below 0.7 ML coverage, C-C and C-H bond cleavages are more favorable than C-O bond cleavage resulting in a total decomposition into CO, H_2 and graphitic carbon. Upon adsorption of Phenol on Rh(111), the multilayer molecularly desorbs at 210 K. Part of the saturated surface undergoes molecular desorption at 240 K and the remaining molecules on the surface decompose into phenoxy via O-H bond cleavage at temperatures below 300 K.[13] The C-H bond cleavage is observed at 350 K and above. Observable products of desorption are CO and H_2. Whereas on Mo(110), the multilayer desorbs at 210 K and a weakly bond layer desorbs at 240 K. Desorption competes with reaction on the surface, where a phenoxy species is formed below 300 K and subsequently decomposes into H_2, surface oxygen and hydrocarbon fragments. All C-O bond cleavages occur by 450 K[14] (no molecular desorption of CO is observed). No formation of benzene has been reported from the decomposition of phenol on Rh(111) or Mo(110). Similarly, on Ni(110) the phenol multilayer desorbs at 200 K and a non-reactive second layer is observed to desorb at 224 K. The first layer totally decomposes into phenoxy between 250-350 K.[10] Further decomposition of phenoxy leads to the formation of H_2 and CO as the only observed byproducts. Those studies demonstrate the intrinsic differences between the first, second and multilayer behavior, and the presence of phenoxy as an intermediate.

Phenoxy also seems to be a key intermediate in the decomposition of more complex oxygenated aromatics.[12,15–17] As an example, Vohs and co-workers and King and co-workers propose the formation of the phenoxy species as the main intermediate for anisole decomposition on Pt(111) and Pt(100)hex.[15,18] Combining surface science experiments and periodic DFT computations,[12] Réocreux et al. showed that anisole on Pt(111) reaches a saturation coverage of one monolayer (1 ML) corresponding to 7 carbon atoms per 10 platinum atoms on the surface, 7C/10Pt. For a coverage below 1 ML, a small fraction of anisole molecularly desorbs from the surface at 360 K while the majority decomposes into phenoxy via a C-H bond cleavage on the methyl group below 325 K. At higher temperatures, there is a competition between Ph-O bond cleavage, forming phenyl then benzene, and a complete decomposition of the aromatic ring. These results showed that under UHV conditions, the formation of benzene is dominant and it desorbs from the surface at 400 K. Above 450 K, the remaining phenoxy completely decomposes into CO and H_2.

Several studies also demonstrated that the introduction of specific additives promotes the decomposition of oxygenated aromatics. Vohs and co-workers have shown that the introduction of Zn to enhance binding through the oxygen group leads to the preferential breaking of the Ph-O bond.[19] A similar behavior was seen for benzaldehyde on Pt(111).[15] On H_2 pre-covered Pt(111), part of the benzaldehyde molecularly desorbs from the surface at 200K while the rest completely decomposes into CO, H_2 and CH_4, keeping the C-O bond intact. In contrast, on H_2 pre-covered Zn/Pt(111), upon heating to 200K, part of the benzaldehyde molecularly desorbs from the surface and part of it reacts by breaking the C-O bond and leads to toluene and other compounds. Due to the bonding of the carbonyl oxygen with Zn sites, the C-O bond cleavage is facilitated. In addition, Medlin's group investigated the interaction of benzyl alcohol on Pt(111) and Pt(111)/Mo surfaces using a combination of TPD experiments and DFT calculations.[20] On clean Pt(111), benzyl alcohol mainly decomposes into benzene, CO and H_2. Here also C-C and C-H bond cleavage are favorable. However, upon depositing benzyl alcohol on the Mo modified Pt(111) surface, the decomposition of benzyl alcohol into benzene, CO and H_2 decreases and the production of toluene is observed. The presence of Mo subsurface atoms decreases the strong adsorption of the aromatic ring on the surface, leading to a change in the adsorption geometry of benzyl alcohol that favors the C-O bond cleavage. This example shows that changing the electronic structure of the Pt(111) surface can influence the adsorption energy and geometry of the aromatic molecules. A less strongly adsorbed aromatic group on the Pt(111) surfaces tends to make C-O bond cleavage accessible. All these examples demonstrate the need for a deoxygenating species on the Pt(111) to break the Ph-O or the C-O bond. In the case of anisole, it has been shown recently that surface carbonaceous species can play this role explaining the formation of benzene under ultra high vacuum conditions[12] in contrast with the selectivity towards phenolics under hydrogenolysis conditions of related molecules.[21–28]

Although the dominant binding of 2-PE to the surface is through the benzene ring, it is expected that at low temperature the aromatic ring remains intact.[11,12,18,29] The early reactivity might therefore be governed by the substituent. In other words, at low temperature, 2-PE can be thought of as a substituted ethanol. The reactivity of such C2 flexible adsorbates (like ethanol or ethylene glycol) has already been reported in the literature.[30,31] Although it depends on both the nature of the surface and the substrate, C-H cleavages are usually rather easy. At a certain dehydrogenation level, the C2 oxygenates can undergo a C-C cleavage. As for the C-O bond, a higher dehydrogenation level is required for the cleavage to proceed on Pt(111).[30,31]

Overall, to understand the different reaction pathways of lignin decomposition, it is important to systematically increase the level of complexity of the model molecules used, as it has recently been reported.[26–28] This work provides a detailed description of the interaction and decomposition pathways of 2-PE on a Pt(111) surface. The focus is on the mutual influence of the arm and the aromatic moiety in regards to the reaction selectivity (in particular, the influence of this flexible oxygenated arm on the Ph-O bond breaking). It will combine detailed DFT calculations with experimental techniques focusing on the 1st layer reactivity of 2-PE on the surface. Experimental results will be presented for X-ray photoelectron spectroscopy (XPS) and

temperature programmed desorption (TPD).

Experimental

Experiments were performed under ultra high vacuum (UHV) in a stainless steel analysis chamber with a base pressure of 5 x 10^{-10} mbar. The Pt(111) crystal surface was cleaned by repetitive cycles of 15 min of sputtering (1.5 keV, 1 x 10^{-5} mbar Ar^{+}) at 600 K, followed by annealing to 1100 K, described in details previously.[12]

2-phenoxyethanol (+99% purity, Sigma Aldrich) was introduced to the UHV chamber through a leak valve that was connected to a gas manifold with an attached 2-PE reservoir. The reservoir was heated to 435 K to increase the vapor pressure and ensure the purity of the deposition. The gas manifold was heated accordingly to prevent condensation and allow a constant, stable flux of 2-PE gas into the chamber. Exposure of 2-PE to the surface was typically performed at 1x10^{-8} mbar pressure and the dosage measured in Langmuirs (1 L = 1.33x10^{-6} mbar ● s).

The carbon coverage was determined by calibration with the C 1s XPS signal of the CO saturation coverage on Pt(111) at 300 K. Under these conditions, CO is known to saturate with a coverage of C/Pt = 0.49 ± 0.02 (1 CO molecule for every 2 Pt atoms).[32] Comparison of this saturation with the intensity dependence of the carbon signal from 2-PE allowed us to determine the amount of deposited carbon per platinum atoms. Every Dosage of 2-PE on Pt(111) and its corresponding C/Pt ratio can be found in table S1 (Supplementary information). We define the coverage as the amount of carbon per Platinum atoms.

XPS

XPS spectra were recorded on a Specs GmbH system (XR50 X-ray source and Phoibos 100 SCD analyzer) using a standard Al Kα source (1486.7 eV) operated at 380 W (14.6 kV, 26 mA). Selected peaks were obtained in high resolution spectra using 0.1 eV step size, 0.5 second dwell time, and pass energy of 20 eV. For the C1s and O1s regions 3 scans were acquired to increase the signal to noise ratio. The spectra were then fit using CasaXPS analysis software using a mixed Gaussian-Lorentzian function and Shirley background subtractions for the C1s region while a Linear background subtraction was used for the O1s region.

For the experiments, 2-phenoxyethanol was dosed on the clean sample at 110 K and then heated up to the desired temperature of observation to acquire the spectrum. Once the acquisition was done, the sample was subject to a cleaning cycle (Ar sputtering followed by annealing to 1100 K) to remove all the residual carbon on the surface. The cleanness of the sample surface was verified by LEED and XPS.

TPD

The TPD experiments require the placing of the sample in front of a differentially pumped quadrupole mass spectrometer (QMS) and ramping up the sample temperature while

monitoring the fragments of interest. For our experiments, the Pt(111) sample was dosed with varying exposures of 2-phenoxyethanol at 110 K and placed 1 mm below a 1 mm diameter hole leading to the differentially pumped QMS. The temperature controlled heating ramp was programmed in LabView and designed to provide and record a linear temperature ramp in the range of 120 K to 800 K, with a ramp rate of 6 K/s. the sample was subject to one cleaning cycle (Ar sputtering followed by annealing to 1100 K) to insure the cleanness of the surface before each dosage. A total of 13 channels corresponding to m/z values of 138, 122, 108, 94, 78, 77, 65, 45, 33, 32, 31, 28 and 2, were monitored for the 2-PE TPD experiments. The selected m/z values correspond to the expected species and their respective fragmentation patterns.

Computation Details

The plane-wave periodic DFT calculations were performed using the Vienna Ab initio Simulation Package (version 5.3).[33–35] The energies were computed using the optPBE[36,37] exchange correlation function that was proven to account accurately for the interactions of aromatics on metal surfaces.[38,39] The core electrons were treated using the Projector Augmented Wave (PAW) method.[40] The valence electron density was developed on a plane wave basis set truncated at 400 eV. All the structures were considered optimized for forces less than 0.02 eV/A.

Unless defined otherwise, four-layer p(4x4) slabs were considered. The Pt atoms of the down most two layers were held fixed at the bulk position. The metallic surface was then surmounted with a 5 layer void (counted in units of Pt interlayers) in order to minimize the unphysical interactions arising from the 3D periodicity of the calculation. The integration over the Brillouin zone was performed using a Γ-centered 3x3x1 Monkhorst-Pack k-point mesh.[41] Gas phase structures were optimized in a 20x20x20 $Å^3$ cell computing the energy at the Γ point only.

Transition state structures were first interpolated from the structures of the reactant and the product using the Opt'n'Path program.[42] They were then pre-optimized using the CI-NEB algorithm[43,44] and finally fully optimized using a quasi-Newton algorithm or the Dimer Method.[45–47]

We performed a frequency calculation for each structure in order to, first, check the first-order saddle point property of the transition states, and second, calculate the Zero-Point Energy correction (ZPE) and the vibrational entropy (calculation at 400 K supposed constant). For slab structures, only the uppermost layer was included in the finite difference scheme of the frequency calculations. The two weakest modes associated to the global horizontal motion of the platinum atoms along the cell vectors were moreover removed before the calculation of the entropic contributions as in our previous work.[12] The rotational and translational entropies (the latter depending on the partial pressure of the gas) were also taken into account for gas phase hydrogen. We assumed for hydrogen a partial pressure of 10^{-10} mbar, corresponding to the order of magnitude of the pressure inside the UHV chamber. It only concerns hydrogen since the partial pressure of the other desorbing products is zero and the associated chemical potential is

therefore ill defined. All the entropic contributions were evaluated using the equations of statistical mechanics for a free particle in a box, a rigid rotator and a harmonic oscillator.

Results and Discussion

(a) XPS and TPD

The identification of surface species upon dosing 2-penoxyethanol on Pt(111) was initially performed by monitoring the carbon and oxygen environment of species on the surface as a function of temperature. Figure 2 shows C 1s and O 1s photoelectron spectra after deposition of 1.5 L of 2-PE on Pt(111) at 110K, with spectra acquired at varying temperatures. Upon deposition, at 120K, 2-PE shows two peaks in the C 1s spectra, one at 285.3 eV, which is attributed to carbon bound to an oxygen atom (labeled C-O), and the other one at 283.5 eV which is attributed to carbon atoms bound only to other carbons or hydrogens (labeled C-C).[11] The binding energy difference between the carbon peaks is 1.8 eV. After flashing to 260K, the C-C and C-O peak areas decrease in intensity as some desorption takes place and only the C-O peak shifts to lower binding energy (285.1 eV). Then, the binding energy difference of the C 1s signals of the C-C and C-O peaks reduces from 1.8 eV to 1.6 eV, suggesting a decomposition of the parent molecule. At 300 K, the C-C and C-O areas decrease in intensity as desorption of the byproducts takes place. At 360K, the C-O peak area vanishes. Upon heating to 460 K, the remaining C1s area peak decreases as only adventitious carbon remains on the surface.

Observations of the O1s region after depositing 1.5L of 2-PE at 110 K on Pt(111) correlates with observations in the C1s region. Upon deposition, at 120 K, 2-PE shows one peak at 532.2 eV. After flashing to 260K, the peak area intensity decreases and shifts to lower binding energy of 531.5 eV as some desorption and decomposition takes place. This is consistent with the observations made on the C1s region. At 300 K, the peak area decreases in intensity as some anisole and phenol start desorbing from the surface (see TPD data below). At 360 K, the peak area vanishes.

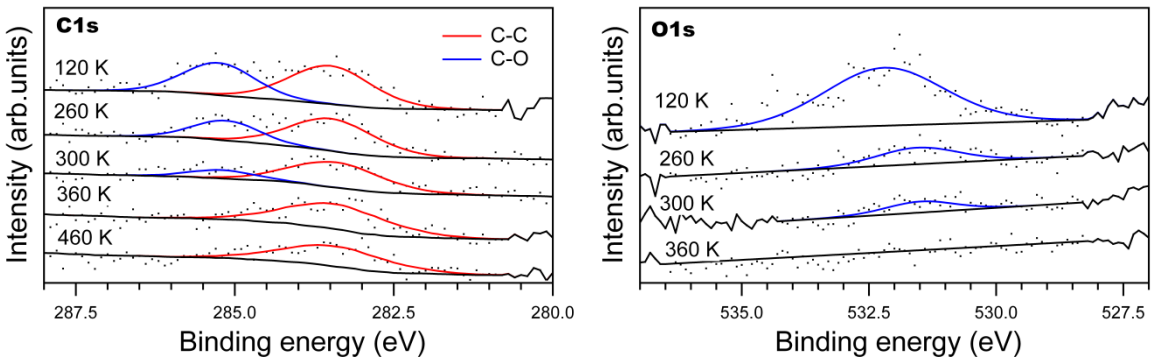

Figure 2: *XPS spectra acquired at different temperatures for 1.5L of 2-phenoxyethanol deposited at 110 K.*

Integrating the area of the C1s region gives insight on how the coverage changes as a function of temperature (Figure 3). A dose of 1.5 L, which corresponds to one molecule of 2-PE per 10 Pt atoms (as determined by XPS intensities, see SI), corresponds to the onset of multilayers on the surface. The large drop in C1s peak area between 240 K and 260 K corresponds to desorption of the multilayer as will be further discussed in comparison with TPD results.

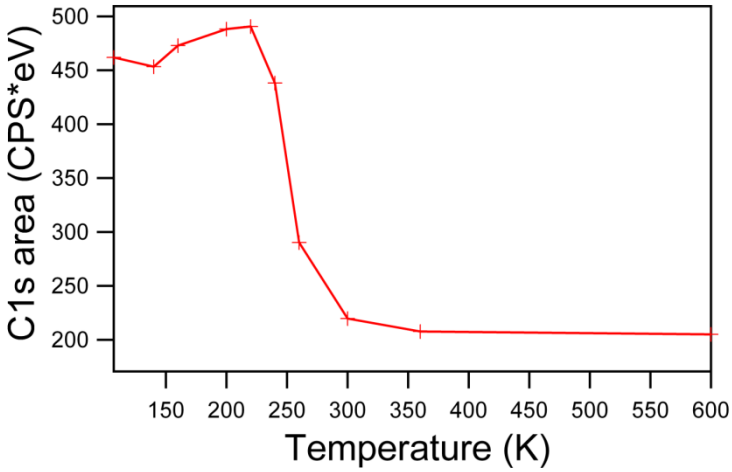

Figure 3: *Analysis of XPS spectra acquired at different temperatures for 1.5L of 2-phenoxyethanol deposited at 110 K. The peak area decreases drastically between 240-260K, which corresponds to desorption of the multilayer.*

Turning now to the TPD experiments, molecular desorption of the parent 2-PE molecule was monitored for multiple coverages as a function of temperature (Figure 4). The data shows no molecular desorption of 2-PE at low coverages (0.85 L and below). As the coverage increases and a dose of 1.12 L is reached, the second layer of 2-phenoxyethanol is seen to molecularly desorb with a peak at 256 K. Assignment of these desorbing molecules to the second layer (rather than generically from multilayers) was made not only by the quantification of molecules, but also by comparison of the desorption energy values with DFT calculations (see below, Figure 8). A low temperature peak appears at 238 K for higher doses and does not saturate within the range of our measurements. This 238 K peak is attributed to the multilayer desorption. Studies on phenol have reported a similar behavior for the multilayer.[10,14]

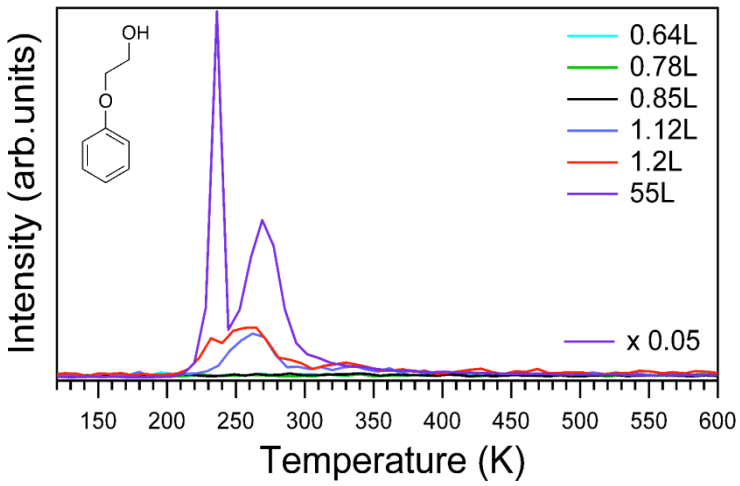

Figure 4: *TPD spectra after several 2-phenoxyethanol exposure at 110K on Pt(111)and desorption rates are measured using a linear temperature ramp of 6 K/s*

Three primary reaction products result from the decomposition of 2-PE on the surface, namely anisole, phenol and benzene. The TPD for these species are shown in Figure 5. By far, the highest intensity was observed for benzene, making it the primary desorbing aromatic product as discussed below. The TPD spectrum for the benzene fragments (mass 78) shows that for 0.78 L coverage, benzene molecularly desorbs from the surface with a peak at 380 K and keeps desorbing up to 520 K. As the coverage increases, the peak centers at 360 K. Phenol and anisole desorb in small quantity in a peak centered at 360 K, but only for initial coverage of 0.85 L or higher. The dosage dependence, particularly the lack of observed desorbing aromatics at lower coverages, is in agreement with previous literature where it was also shown that aromatics such as benzene, phenol and anisole decompose completely on the Pt(111) surface for coverages below 0.6 ML.[11,12,48,49]

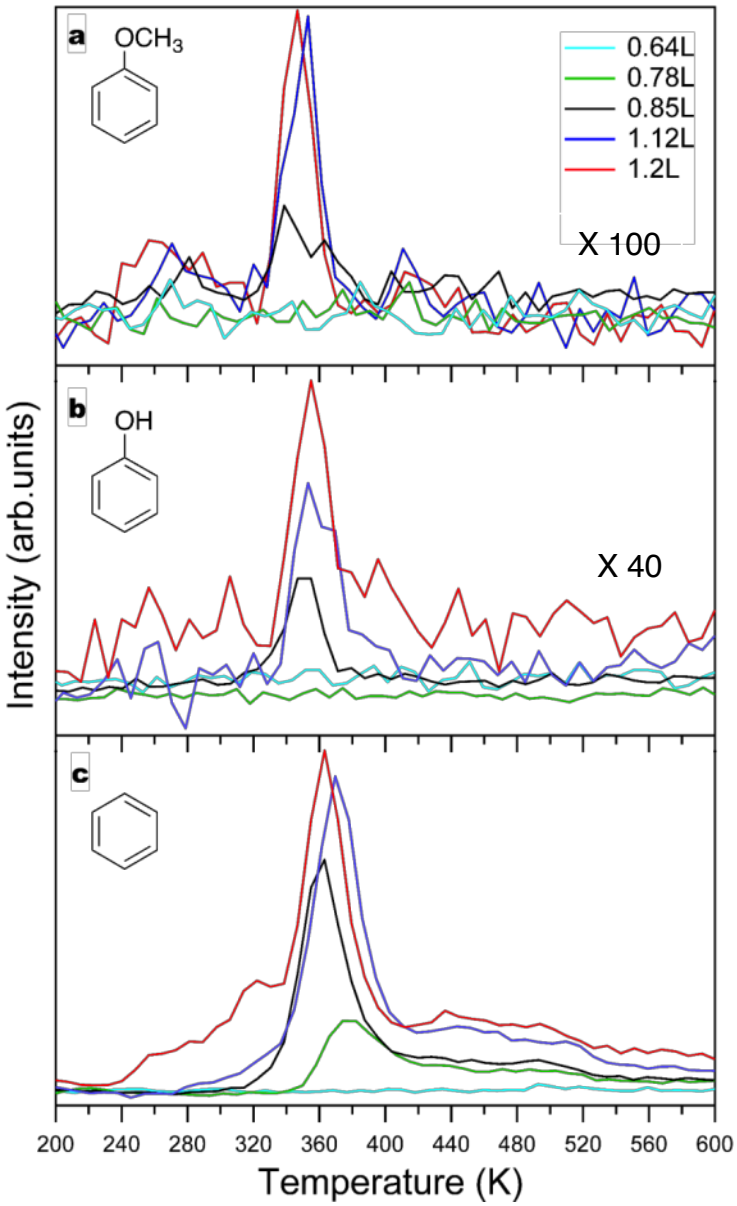

Figure 5: *TPD spectra after several 2-phenoxyethanol exposures at 110K on Pt(111). Monitored masses 108, 94 and 78 correspond to Anisole, Phenol and Benzene respectively. The contribution of the parent molecule from the fragmentation pattern in the gas phase has been subtracted so as to show only desorbing species (see SI for subtraction procedure). Desorption rates are measured using a linear temperature ramp of 6 K/s.*

The only other observed reaction products of the decomposition of 2-PE are H_2 and CO (Figure 6). Hydrogen shows peaks at 334 K, 438 K and 555 K with two shoulders at 357 K and 520 K after dosing 0.85 L of 2-PE. For comparison, the associative desorption of hydrogen from Pt(111) has been previously observed in the temperature interval between 290-375 K.[50,51] The

dot-dash line in Figure 6, which matches the observed peak in these experiments, corresponds to the reported dosage of 2L of H_2 on clean Pt(111).[50] Above 375 K the hydrogen peaks might correspond to the decomposition of the phenoxy species on the surface as observed with phenol and anisole on Pt(111).[11] The additional high temperature hydrogen peaks in Figure 6 have been assigned to subsequent surface reactions yielding H_2 as a product. In an attempt to quantify the origin of the hydrogen products, fitted Gaussians have been used to estimate the area ratio between the desorption peaks (see SI). The desorption spectra can be fitted with 5 peaks (centered at 335 K, 357 K, 438 K, 520 K, and 554 K respectively) with a corresponding area ratio of approximately 2:1:5:1:1. This qualitative ratio, normalized to the smallest peak as 1, correlates with the number of 10 hydrogen atoms in the 2-PE molecules. The corresponding sequence of dehydrogenation will be discussed below using DFT calculations.

In contrast with the rich hydrogen spectra, only one broad peak of CO is observable at 404K with a shoulder at 438K. The dashed line for CO corresponds to molecular desorption of pure CO from Pt(111) with 0.5ML coverage.[52] No other molecular products have been observed.

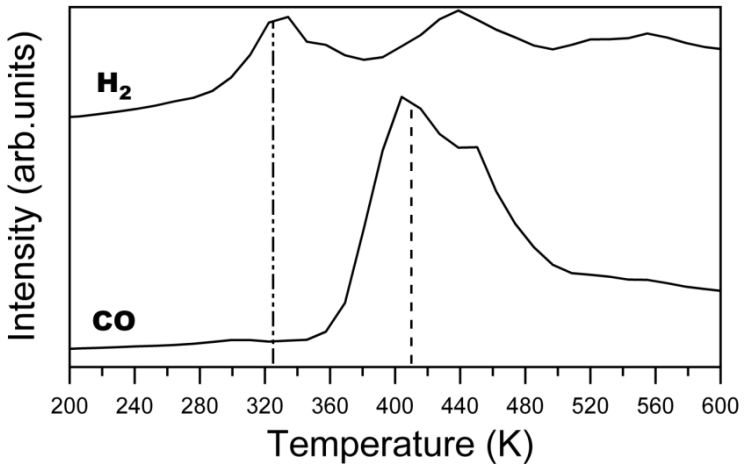

Figure 6: *TPD spectra after 0.85L exposure of 2-phenoxyethanol on Pt(111) and selecting formed byproducts Hydrogen and Carbon-monoxide (Mass 2 and 28). Desorption rates are measured using a linear temperature ramp of 6 K/s. The dashed line for CO corresponds to molecular desorption of pure CO from Pt(111) with 0.5ML coverage.*[52] *The dot-dashed line for H_2 corresponds to desorption temperature of Hydrogen with 2L coverage from Pt(111).*[50,51]

Analysis of the TPD data allows the experimental determination of desorption energies E_{des} for each species and it can also provide information on the activation energy associated with surface reactions (Table 1). The analysis is performed based on the general rate law for

desorption by the simple approach of Redhead[53] with appropriately corrected frequency factors. The calculated frequency factors **ν** are presented in Table 1 as obtained using the Campbell approach for molecular or associative desorption[54–56] and temperature corrected entropy values from the Yaw's Handbook.[57,58] The only exception is for 2-phenoxyethanol, where the entropy value for anisole was used as an approximation (the entropy value for 2-phenoxyethanol is not available). Further details on the choice of the approach method have been previously described.[12]

The high temperature peaks in the hydrogen TPD spectrum correspond to H_2 generated at a temperature above its normal desorption temperature and hence the associated activation energy calculated corresponds to the process that generates the additional H atoms. This quantity is labeled as the apparent activation energy E_a^{app}.

Table 1: *Desorption energies of observed species, calculated by Redhead analysis of the TPD data.*

Species	**Observations**	**Temperature (K)**	**ν^a (s^{-1})**	**E_{des} (kJ/mol)**	**E_a^{app} (kJ/mol)**
2-phenoxyethanol	2nd Layer	256	5.4×10^{16}	81	-------
	Multilayer	238	3.5×10^{16}	75	-------
Anisole	Molecular desorption	355	2.2×10^{17}	119	------
	Literature				-------
	2nd layer	260[12]	5.4×10^{16}	83	-------
	saturated 1st layer	360[12]	2.4×10^{17}	121	
Phenol	Molecular desorption	355	3.9×10^{16}	-------	114
	Literature	225[11]	-------	57	-------
Benzene	Molecular desorption	363	8.0×10^{15}	112	-------
		510	2.2×10^{18}	182	
	Literature	400-550[49]	-------	133-200[48]	-------

Carbon monoxide	Molecular desorption	404	7.7×10^{14}	117	-------
		438	8.5×10^{14}	128	
	Literature	410[59]	-------		-------
Hydrogen	Analyzed as molecular desorption	335	1.9×10^{14}		93
		357	1.9×10^{14}		100
		438	2.0×10^{14}		123
		520	2.1×10^{14}		147
		554	2.1×10^{14}		157
	Analyzed as associative desorption	335	1.05×10^{9}	-------	54
		357	9.92×10^{8}	-------	58
		438	8.62×10^{8}	-------	72
		520	7.66×10^{8}	-------	85
		554	7.20×10^{8}		91
	Literature	293-375[50]	-------	-------	39.7[50]
		330[51]	-------	-------	73[51]

Since decomposition of 2-phenoxyethanol and its fragments is significant, even at relatively low temperatures, we have quantified the amount of carbon left on the surface at different stages using the C1s XPS signal. Figure 3 shows an example of the C 1s intensity upon dosage of 1.5 L of 2-phenoxyethanol and the decrease in signal due to multilayer desorption, yielding a residual carbon signal corresponding to decomposition species. To assess the relative yield of the decomposition vs intact desorption pathways during reaction, the C 1s intensity for one monolayer had to be estimated. This was done by comparison of the XPS signal for several doses as well as by determination of the XPS intensity at a temperature where the multilayer has desorbed (as determined by TPD). In Figure 3, the monolayer intensity was determined at T=260K (lowest temperature to allow second layer desorption prior to XPS data collection) and the residual carbon intensity at T=360K. From this analysis, it was determined that

approximately 29% of the monolayer desorbs as molecular fragments, while 71% decompose into carbonaceous species.

Now getting back to the TPD data, one can correlate the peak area of the desorbing fragments to the amount of desorbed byproducts (see Table 2). At low coverages such as 0.64 L, 1 molecule per 23 Pt atoms (C/Pt=8/23), no desorption of byproducts is observed. The decomposition of the aromatic ring in 2-phenoxyethanol is dominant due to the availability of many unoccupied sites. At 0.78 L, 1 molecule per 19 Pt atoms, only benzene is observed as a byproduct. As the carbon coverage on the surface increases to 1 molecule per 16 Pt atoms (0.85 L), a competitive reaction pathway is observed with desorption of phenol and anisole. As the surface gets more crowded, part of the Ph-O bond cleavage is inhibited. The ratio of desorption of the byproducts is maintained at a higher coverage of 1 molecule per 12 Pt atoms (1.2L).

Table 2: *Analysis of the TPD spectra after different dosages of 2-phenoxyethanol on Pt(111) at 110K. As the carbon coverage increases anisole and phenol desorption is observed.*

Exposure (L)	Molecule/Pt	Anisole (%)	Phenol (%)	Benzene (%)
0.64	1/23	0	0	0
0.78	1/19	0	0	100
0.85	1/16	0.2	4.8	95
1.12	1/13	0.1	6	93.9
1.20	1/12	0.3	6.5	93.2

(b) Proposed pathway combining XPS and TPD.

From XPS and TPD experimental results, a schematic of the reaction and decomposition of 2-phenoxyethanol on Pt(111) is proposed in Figure 7. Upon dosing, 2-phenoxyethanol adsorbs on the Pt(111) surface at 110 K. Then, when heating, the multilayer molecularly desorbs at 238 K followed by desorption of the 2nd layer at 254 K. The desorption energies are measured as 75 kJ/mol for the multilayer in reasonable agreement with the enthalpy of vaporization of 66 kJ/mol[58] of 2-phenoxyethanol, and 81 kJ/mol for the second layer molecules in good agreement with the DFT calculated adsorption energy of 85 kJ/mol (see below, Figure 8).

The first saturated layer totally decomposes on the surface. The only observed byproducts are anisole, phenol, benzene, CO and H_2. At 260K, the C 1s binding energy difference between the C-C and C-O XPS peaks reduces to 1.65 eV, suggesting the onset of decomposition of the parent molecule. This is comparable with the difference of 1.6 eV and 1.7eV C 1s binding energy of pure anisole and phenoxy on Pt(111)[11,12] suggesting these two species may be produced on the surface. The associative desorption of H_2 at 335K (which corresponds to "usual'

temperature desorption of H_2) is another clear indication of the decomposition of the parent molecule. Literature suggests that this first hydrogen desorption comes from the cleavage of the O-H bond,[10,11,13,14] but a more detailed discussion of the origin of H at the different stages of reaction will be explored using mechanistic DFT calculations. Upon heating to 360 K, aromatics derived from the 2-phenoxyethanol, start to desorb: traces of anisole, few percent of phenol and a majority as benzene. Anisole is known to decompose into phenoxy and to yield benzene and not phenol, as its been reported in a previous study.[12] Thus, the benzene that starts desorbing at 363K could be obtained through the following sequence: C-C bond breaking, generation of anisole and/or phenoxy, decomposition into benzene.

The additional presence of non-negligible amount of phenol questions the role of the glycoxy arm in the selectivity of the decomposition. Since phenol completely decomposes in the first layer before reaching its desorption temperature,[11] the observed phenol from 2-PE decomposition must be formed at a temperature that is higher than its desorption temperature. Therefore, the observed molecular desorption of phenol at 355 K has to be reaction limited, that is, as soon as it is formed it already has enough energy to desorb and hence the measured E_a^{app} should be comparable to the activation energy of the reaction that produces it. Desorption of oxygen containing species (anisole, phenol, carbon monoxide, etc.) correlates with the disappearance of the C-O peak in C1s and in the O1s region at 360 K and only hydrocarbons and adventitious carbon remains on the surface at 460 K.

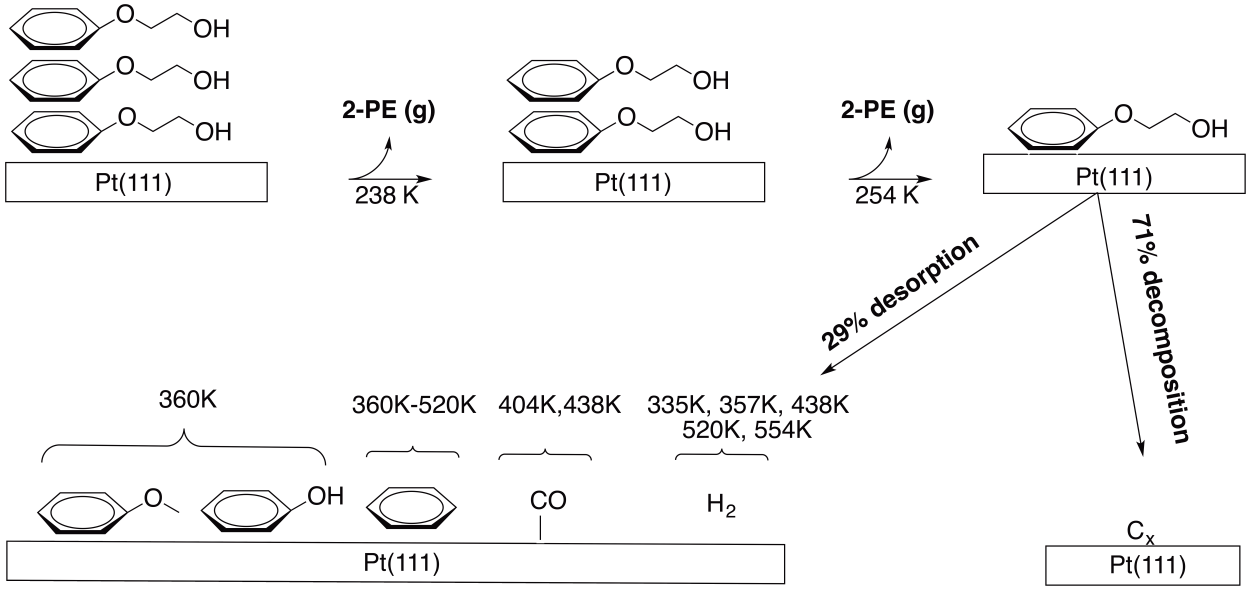

Figure 7: *Proposed pathway of 2-phenoxyethanol (2-PE) decomposition under UHV conditions on Pt(111) built form surface science experiments (the temperatures correspond to the TPD peaks).*

To achieve additional insight into the selectivity toward the different bond cleavage mechanisms (shown in Figure 1) involved in 2-phenoxyethanol decomposition on Pt(111), the different reaction steps associated with the experimentally obtained pathway (Figure 7) have been calculated. In the following section, we use periodic DFT calculations to not only corroborate some of the experimental conclusions, but also to propose the reasons for the formation of benzene, phenol and anisole as products and particularly for the coverage dependence of their appearance.

(c) Mechanistic insight from DFT calculations

i. 2-phenoxyethanol (2-PE) desorption

TPD experiments show that the molecular desorption of 2-PE occurs at both 238 K and 256 K (see Table 1) at a dosage above 1.12L. To assess the structure in function of coverage, the adsorption structure and energy are computed on different sized slabs (see Figure 8). The most stable structure on the p(4x4) slab is found at the bri30 site in agreement with our previous study on the adsorption of oxygenated aromatics on Pt(111)[60] and with previous studies on related adsorbates.[12,26,27,61,62] The desorption energy at such a coverage (1 molecule : 16 Pt) is computed at 200 kJ/mol, much larger than the one expected from the TPD (see Table 1, 81 kJ/mol). The structure expands on three Pt atoms in one direction and four in the other one (12 Pt atoms in total) suggesting that this structure – on the 16 Pt atoms of a p(4x4) slab – does not model a saturated monolayer of 2-phenoxyethanol. We were able to put this adsorbate on a smaller p(3x3) slab (9 Pt atoms). The desorption energy decreases to 175 kJ/mol. This coverage effect can safely be attributed to the increased lateral interactions and the reorganization of the glycoxy substituent that has to fit in this smaller p(3x3) cell. In spite of the increased coverage, the interaction of the adsorbate with the metallic surface remains very strong and desorption appears as being a very unlikely process. Increasing the coverage to the second layer gave a desorption energy of 85 kJ/mol. This was modeled using a p(3x3) slab with an extra molecule on top of a chemisorbed 2-PE. For this calculation only, the void thickness was increased to 14 layers (in units of Pt layers). For the second layer, only weak physical interactions ensures the stability of the two-layered system which explains why the desorption energy has been more than halved on going from the first to the second layer. The calculated value of 85 kJ/mol matches well with the desorption energy obtained experimentally (see Table 1, 81 kJ/mol). Consequently, it is the first layer, which cannot desorb, that contributes most significantly to subsequent reaction products.

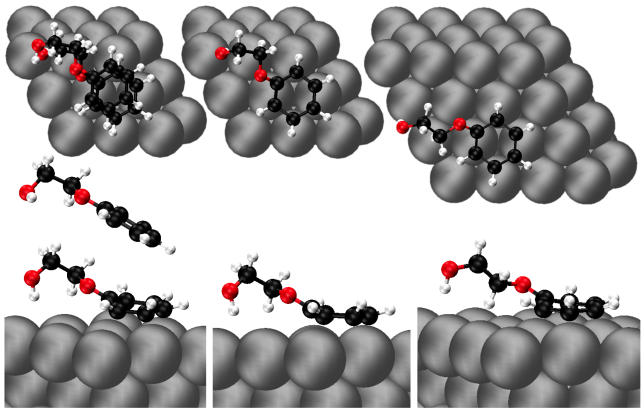

Figure 8: *Adsorption geometries of 2-phenoxyethanol at different coverages on Pt(111) (M designates the number of organic molecules and Pt the number of surface platinum).*

ii. Low coverage reactivity

Since it is extremely complex to tackle coverage effects for coverages close to saturation using only DFT and geometry optimization (many very specific geometrical configurations would need to be tested), we focused on the reactivity study using the large enough p(4x4) slab on which the lateral interactions are not too important and less likely to be specific.

2-PE has twenty bonds and as many first reactions possible. This means that there is, in principle, a very large reaction network to study. However, from previous experimental and theoretical studies, it is known that the first bonds to be broken are unlikely to be on the aromatic moiety, without yielding coke.[11,12] In other words, although the dominant binding of 2-PE to the surface is through the benzene ring, in terms of initial reactivity we can think of the molecule as a phenoxy substituted ethanol. Comparing the substituent to the numerous studies on oxygenated C2 organic compounds suggests that the C-C and C-O bonds cannot be cleaved unless a certain level of dehydrogenation has been reached.[30,31] Therefore, the early reactivity should be governed by C-H and O-H cleavages. Among the O-H and C-H bonds (see Table 3 for the activation parameters), the α hydrogen appears as being the easiest cleavage in ethanol ($\Delta^{\ddagger}U$=58 kJ/mol). In 2-PE however, this is the most recalcitrant to abstraction with a barrier of $\Delta^{\ddagger}U$=119 kJ/mol. This difference in activation energies ($\Delta\Delta^{\ddagger}U$=61 kJ/mol) illustrates that the adsorption through the aromatic moiety can exert a strong constraint on the reactivity of the C2 fragment; and this, in spite of the distance of the C_{α} carbon to the aromatic group. In the transition state of ethanol dehydrogenation, the C_{α} is on top of a Pt atom at a height of 2.63 Å from the surface (see Figure 9) and can easily take the ideal and classic triangular shape. Because of the phenoxy group that acts as a real anchor at the bri30 site, 2-PE does not have the same capability to adapt to this 3-center transition state. Although the C_{α} manages to get even closer to the surface (2.57 Å), it does not lie over a Pt atom and the hydrogen reaches a bridge position, in a strongly distorted 4-center transition state. Despite a reduce distance between the aromatic and the C_{β}, the C_{β}-H is impacted to a lesser extent ($\Delta\Delta^{\ddagger}U$=28 kJ/mol). The corresponding transition state

appears as less strained since it manages to reach the stable 3-center configuration (see Figure 10). Lastly, the O-H bond seems to be less impacted energetically ($\Delta\Delta^{\ddagger}U$=9 kJ/mol) than entropically ($\Delta\Delta^{\ddagger}S$=-46 $J.K^{-1}.mol^{-1}$). Unlike ethanol, which directly interacts via its oxygen in both the initial state and the transition state, 2-PE indeed undergoes a bigger conformation restriction from a free –OH group to the 4-center transition state (see Figures 8 and 10).

In short, the 2-PE decomposition starts with the O-H scission. This detailed comparison between the 2-PE and the simple ethanol molecule shows that the bond scission in the pending arm can be strongly affected by the presence of the aromatic moiety, and that they are systematically destabilized. In the following analysis of the reaction network, this will be used as a general behavior to avoid exploring the entire reaction network.

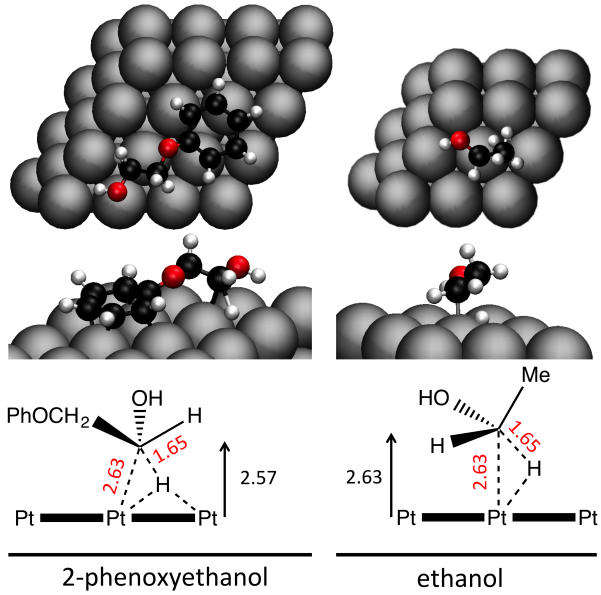

Figure 9: *Structures of the transition states associated to the C_{α}-H cleavage on 2-phenoxyethanol (left panels) and ethanol (right panels). Distances are reported in Å.*

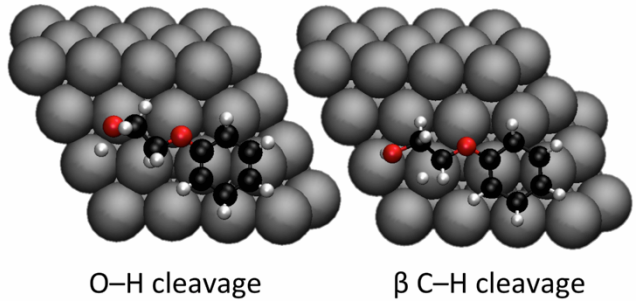

Figure 10: *Structures of the transitions states associated to the O-H and C_{β} -H cleavages on 2-phenoxyethanol.*

Table 3: *Comparison of the reactivity of ethanol and 2-phenoxyethanol (2-PE) for the different O-H and C-H cleavages. These DFT data were computed on a p(4x4) slab for 2-PE and a p(3x3) slab for ethanol*

	2-phenoxyethanol		Ethanol	
	$\Delta^{\ddagger}U$ ($kJ.mol^{-1}$)	$\Delta^{\ddagger}S$ ($J.K^{-1}.mol^{-1}$)	$\Delta^{\ddagger}U$ ($kJ.mol^{-1}$)	$\Delta^{\ddagger}S$ ($J.K^{-1}.mol^{-1}$)
O-H	84	− 65	75	−19
C_{α}-H	119	−19	58	−10
C_{β}-H	112	−10	84	−31
PhO-C & C_{α}-H	129	+2	—	—

The reaction profile of the 2-PE decomposition is reported in Figure 11, free energy F being computed at 400K. As detailed above, the first step is the breaking of the O-H bond. With a barrier of 110 kJ/mol, it easily competes with the desorption of 2-PE at low coverage. This first process is quite endergonic ($\Delta_r F$=+65 kJ/mol) but is readily followed by the desorption of hydrogen ($\Delta_r F$=-40 kJ/mol), pushing the dehydrogenation forward and making the reverse process unlikely. The subsequent α-dehydrogenation reaction is indeed very slightly activated ($\Delta^{\ddagger}F$=26 kJ/mol) and happens selectively compared to the backward reaction ($\Delta^{\ddagger}F$=85 kJ/mol) and the β-dehydrogenation ($\Delta^{\ddagger}F$=125 kJ/mol). The result of the dehydrogenation at the O-H and C_{α}–H sites affords the corresponding aldehyde (2-phenoxyethanal in conformation A, Figure 12) and hydrogen {$PhOCH_2CHO+H_2(g)$} at F=-71 kJ/mol (see Figure 11). The subsequent α and β dehydrogenations ($\Delta^{\ddagger}F$=73 kJ/mol and 98 kJ/mol respectively) cannot compete with the conformational change to a second conformer labeled B (see Figure 12). This conformational change is admittedly slightly endergonic ($\Delta_r F$=14 kJ/mol) but proceeds though a low barrier of 45 $kJ.mol^{-1}$. In addition B is very reactive towards the second α-dehydrogenation with a barrier of only $\Delta^{\ddagger}F$=31 k/mol (*ie* an overall barrier of $\Delta^{\ddagger}F$=45 kJ/mol from conformer A). As a consequence of the Curtin-Hammett principle, we obtain 2-phenoxyacetyl $PhOCH_2CO$ in a B conformation. After desorption of hydrogen, this step (at F=−149 kJ/mol in Figure 11) becomes irreversible with a reverse barrier of $\Delta^{\ddagger}F$=133 kJ/mol.

The 2-phenoxyacetyl appears as a key intermediate along the reaction path. After the large amount of hydrogen released (3 atoms for one 2-PE molecule), further dehydrogenation appears as kinetically blocked ($\Delta^{\ddagger}F$=160 kJ/mol). In line with the reactivity of ethanol[30] and anisole,[12,15,18] the cleavage of the PhO-C and C-C bonds should be now affordable. The barriers are $\Delta^{\ddagger}F$=92 kJ/mol and $\Delta^{\ddagger}F$=116 kJ/mol respectively, suggesting that the PhO-C cleavage is the most accessible. The products are the phenoxy fragment PhO and the ketene CH_2CO that further decomposes into methylene CH_2 and adsorbed carbon monoxide CO with a barrier of $\Delta^{\ddagger}F$=86 kJ/mol. Further, methylene readily evolves into methylidene CH (see gray part of the diagram) yielding an additional H atom. Then methylidene (or carbon after an extra dehydrogenation step) can snatch the oxygen atom from phenoxy to produce benzene with an overall barrier of $\Delta^{\ddagger}F$=135 kJ/mol around 400 K, as we have recently shown for the anisole/Pt(111) system.

Overall, the production of {PhO+CH+2CO+2H_2(g)} can be considered to proceed with a relatively low overall barrier of $\Delta^{\ddagger}F$=110 kJ/mol and should therefore appear at moderate temperatures under TPD conditions (in the 320-380 K range). It is associated to four dehydrogenations directly followed by hydrogen desorption (see downward arrows in Figure 11). Although, the last dehydrogenation might be a bit delayed by two barriers of $\Delta^{\ddagger}F$=92 kJ/mol and $\Delta^{\ddagger}F$=86 kJ/mol (the associated transition states of which being at F=−57 kJ/mol and F=−118 kJ/mol respectively in Figure 11) to afford methylene CH_2. If the decomposition of 2-PE followed the mechanism proposed in Figure 11 with a selectivity of 100%, one would expect a ratio of approximately 3:1 for the first two peaks in the TPD of H_2 in the 300-400 K range. However, the DFT calculations have shown that the C_{β}-H cleavage, although not preferential, is also possible for the first dehydrogenation ($\Delta^{\ddagger}F$ = 116 kJ/mol at 400 K, calculated from the data given in Table 3). This might open a competitive route that could alter the 3:1 ratio, potentially leading to an observed TPD ratio of approximately 2:1 (Figure 6). At higher temperature, the production of benzene competes with the decomposition of PhO, which can decompose into carbonaceous species initiated by the C-H bond cleavage as shown previously.[48,62] This explains the large production of hydrogen and the shoulder in CO above 400K.

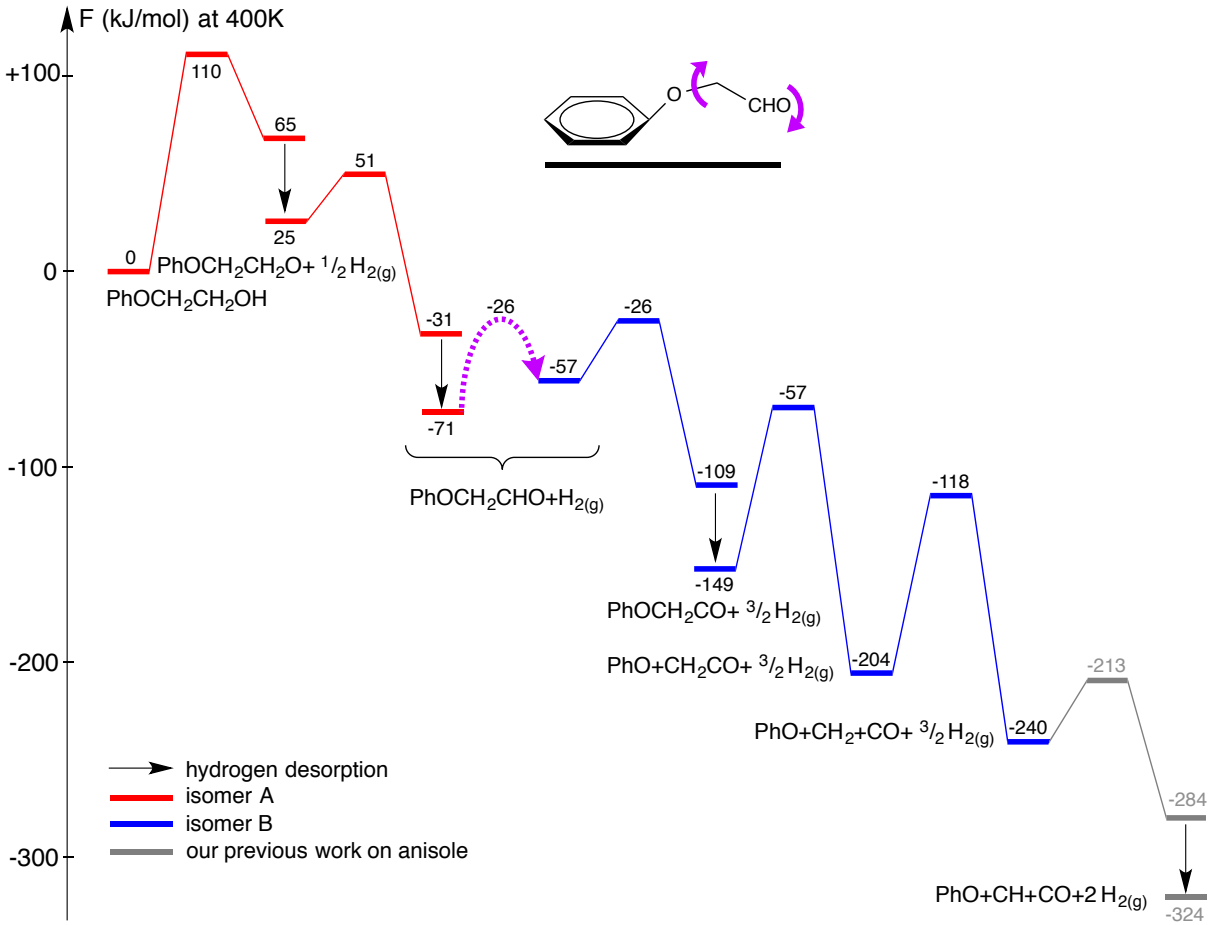

Figure 11: *Free Energy profile of 2-phenoxyethanol decomposition into phenoxy, methylidene, carbon monoxide, and gas phase hydrogen. The free energy was computed at 400 K as described in Computational Details.*

(iii) Towards higher coverages

The proposed mechanism has been derived for low to moderate coverages. However, the TPD experiments show that an increase in the coverage (up to 1 molecule per 12 Pt) yields to a small production of phenol (PhOH) and negligible traces of anisole (see Table 2). The increase of the coverage is expected to favor steps that require a reduced amount of surface Pt at the expense of steps that necessitate more.

The first transition state, corresponding to the dehydrogenation of the alcohol has a geometry where 2-phenoxyethanol lies down on three Pt atoms in one direction and four on the other (see Figure 10). This means that approximately twelve Pt atoms are needed for this step to proceed easily. If the coverage increases, the energy of this transition state should increase. At higher coverages, 2-phenoxyethanol might even lack space to have the alcohol function interact with the surface.

So far, only classic sequential cleavages were considered, following the Langmuir-Hinshelwood mechanism for surface reactions. However, at high coverage, an Eley-Rideal mechanism could be more favorable, the bond cleavage being synchronous with the ejection of one of the products. The simultaneous cleavage of the PhO-C and the C_α-H bonds produces phenoxy PhO, hydrogen and the hydroxyethylene (CH_2CHOH) that is directly ejected in the gas phase (see Figure 13). The free energy barrier is $\Delta^{\ddagger}F$=128 kJ/mol at 400 K on a p(4x4) slab (calculated from the data given in Table 3, entry PhO-C & C_α-H). This barrier is too high to be relevant at low coverages. However, the ejection of the enol makes this alternative competitive at higher coverages with the increase of the other barriers. It leaves locally only phenoxy and hydrogen. In absence of CH_x species, the deoxygenation is unlikely since the Ph-O bond dissociation in phenoxy is highly endothermic ($\Delta_r F$=124 kJ/mol at 400 K). Then, the hydrogen surface diffusion is hindered by the high surface coverage, opening the door to the PhO+H recombination into PhOH instead of {PhO+½H_2(g)}, which would lead to the small yield of phenol observed.

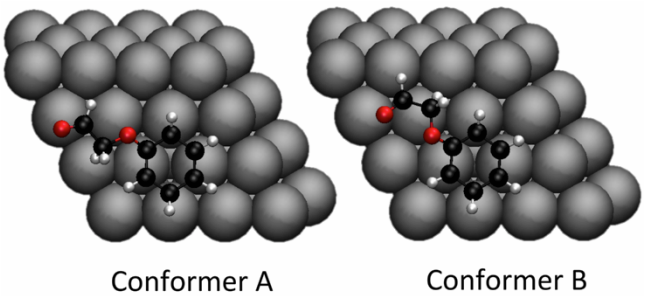

Figure 12: *conformers A & B of 2-phenoxyethanal.*

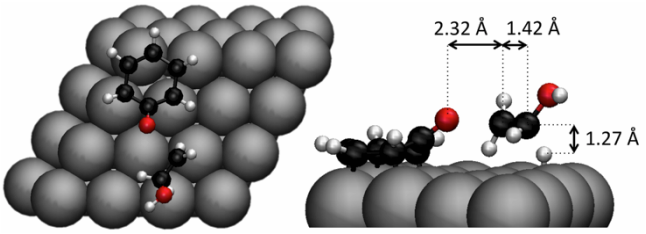

Figure 13: *Transition state structure associated to the concerted formation of enol.*

Conclusion

In ultra-high vacuum conditions, the 2-phenoxyethanol (2-PE) desorbs from the Pt(111) surface in two stages: (i) desorption of the multilayer (ii) desorption of the second layer. The strongly chemisorbed first layer decomposes in coke (71%) and aromatic compounds (29%). The decomposition of the pending arm and the deoxygenation of the aromatic moiety is effective since the main product is benzene and only ~5% of phenol is observed at a higher coverage.

Despite its flexibility, the pending arm of 2-PE is highly constrained by the strong adsorption of the aromatic ring and it does not react as a simpler alcohol such as ethanol. The reaction starts with the O-H scission, followed by two successive C_α-H scissions, yielding the $PhOCH_2CO$ intermediate and 3/2 H_2(g). The alkyl arm of this intermediate cannot be easily dehydrogenated further and undergoes a C-C scission. Falling back to the reaction network of the anisole decomposition, the phenoxy intermediate is obtained and yields benzene thanks to the presence of numerous carbonaceous species.

A higher coverage yields to a higher fraction of oxygenated aromatics (mainly phenol). The DFT calculations suggest that this can be related to the existence of a synchronous step that does not require the adsorption of all the products. The CH_2CHOH fragment is ejected in gas phase as a stable molecule, leaving behind the phenoxy intermediate and one hydrogen atom. Locally, without CH_x species, the deoxygenation is unlikely. In addition, the higher coverage probably limits the H diffusion, allowing the recombination into phenol.

This study opens the road to a better design of metallic based catalysts aiming at lignin deoxygenation.

Supporting Information

Table of surface carbon coverage and its corresponding exposure

Integrated peak of the background Hydrogen contribution

Integrated peaks of TPD of Hydrogen at 0.85 L exposure

Raw TPD data without correction for fragmentation of species in the mass spectrometer

Structures of all the intermediates and transitions states directly related to 2-phenoxyethanol reactivity provided in the *structures.xyz* file.

Acknowledgements

The authors are thankful to the LIA FunCat for its financial support. They also thank the Centre Blaise Pascal (CBP) and the Pôle Scientific de Modélisation Numérique (PSMN), both at the École Normale Supérieure de Lyon, for the computational resources and technical support. JBG thanks the Natural Sciences and Engineering Research Council of Canada for funding.

Author Information

Corresponding authors:

CM email: Carine.michel@ens-lyon.fr

JBG email: Javier.giorgi@uottawa.ca

References

(1) Popp, J.; Lakner, Z.; Harangi-Rákos, M.; Fári, M. The Effect of Bioenergy Expansion: Food, Energy, and Environment. *Renew. Sustain. Energy Rev.* **2014**, *32*, 559–578.

(2) Peter, M. Energy Production from Biomass (part 1): Overview of Biomass. **2002**, *83*, 37–46.

(3) Pettersen, R. The Chemical Composition of Wood. *Chem. solid wood* **1984**, 1–9.

(4) Zakzeski, J.; Bruijnincx, P. C. A.; Jongerius, A. L.; Weckhuysen, B. M. The Catalytic Valorization of Ligning for the Production of Renewable Chemicals. *Chem. Rev.* **2010**, *110*, 3552–3599.

(5) Ragauskas, A. J.; Beckham, G. T.; Biddy, M. J.; Chandra, R.; Chen, F.; Davis, M. F.; Davison, B. H.; Dixon, R. a; Gilna, P.; Keller, M.; et al. Lignin Valorization: Improving Lignin Processing in the Biorefinery. *Science* **2014**, *344*, 1246843.

(6) Pandey, M. P.; Kim, C. S. Lignin Depolymerization and Conversion: A Review of Thermochemical Methods. *Chem. Eng. Technol.* **2011**, *34*, 29–41.

(7) Huber, G. W.; Iborra, S.; Corma, A. Synthesis of Transportation Fuels from Biomass: Chemistry, Catalysts, and Engineering. *Chem. Rev.* **2006**, *106*, 4044–4098.

(8) Mohan, D.; Pittman, C. U.; Steele, P. H. Pyrolysis of Wood/biomass for Bio-Oil: A Critical Review. *Energy and Fuels* **2006**, *20*, 848–889.

(9) Bridgwater, a. V. Review of Fast Pyrolysis of Biomass and Product Upgrading. *Biomass and Bioenergy* **2012**, *38*, 68–94.

(10) Russell, J. N.; Sarvis, S. S.; Morris, R. E. Adsorption and Thermal Decomposition of Phenol on Ni(110). *Surf. Sci.* **1995**, *338*, 189–203.

(11) Ihm, H.; White, J. M. Stepwise Dissociation of Thermally Activated Phenol on Pt(111). *J. Phys. Chem. B* **2000**, *104*, 6202–6211.

(12) Réocreux, R.; Ould Hamou, C. A.; Michel, C.; Giorgi, J. B.; Sautet, P. Decomposition Mechanism of Anisole on Pt(111): Combining Single-Crystal Experiments and First-Principles Calculations. *ACS Catal.* **2016**, *6*, 8166–8178.

(13) Xu, X.; Friend, C. M. The Role of Coverage in Determining Adsorbate Stability: Phenol Reactivity on rhodium(111). *J. Phys. Chem.* **1989**, *93*, 8072–8080.

(14) Serafin, J. G.; Friend, C. M. Carbon-Oxygen Bond Strength as a Control of Reaction Kinetics: Phenol on Mo(110). *Surf. Sci.* **1989**, *209*, 163–175.

(15) Shi, D.; Vohs, J. M. Lignin-Derived Oxygenate Reforming on a Bimetallic Surface: The Reaction of Benzaldehyde on Zn/Pt(111). *Surf. Sci.* **2016**, *650*, 161–166.

(16) Bonalumi, N.; Vargas, A.; Ferri, D.; Baiker, A. Theoretical and Spectroscopic Study of the Effect of Ring Substitution on the Adsorption of Anisole on Platinum. *J. Phys. Chem. B* **2006**, *110*, 9956–9965.

(17) Bonalumi, N.; Vargas, A.; Ferri, D.; Bürgi, T.; Mallat, T.; Baiker, A. Competition at Chiral Metal Surfaces: Fundamental Aspects of the Inversion of Enantioselectivity in Hydrogenations on Platinum. *J. Am. Chem. Soc.* **2005**, *127*, 8467–8477.

(18) Tan, Y. P.; Khatua, S.; Jenkins, S. J.; Yu, J.-Q.; Spencer, J. B.; King, D. a. Catalyst-Induced Changes in a Substituted Aromatic: A Combined Approach via Experiment and Theory. *Surf. Sci.* **2005**, *589*, 173–183.

(19) Shi, D.; Arroyo-Ramírez, L.; Vohs, J. M. The Use of Bimetallics to Control the Selectivity for the Upgrading of Lignin-Derived Oxygenates: Reaction of Anisole on Pt and PtZn Catalysts. *J. Catal.* **2016**, *340*, 219–226.

(20) Robinson, A. M.; Mark, L.; Rasmussen, M.; Hensley, J. E.; Medlin, J. W. Surface Chemistry of Aromatic Reactants on Pt and Mo-Modified Pt Catalysts. *J. Phys. Chem. C* **2016**, *in review*.

(21) Nimmanwudipong, T.; Runnebaum, R. C.; Block, D. E.; Gates, B. C. Catalytic Conversion of Guaiacol Catalyzed by Platinum Supported on Alumina: Reaction Network Including Hydrodeoxygenation Reactions. *Energy & Fuels* **2011**, *25*, 3417–3427.

(22) Runnebaum, R. C.; Nimmanwudipong, T.; Block, D. E.; Gates, B. C. Catalytic Conversion of Anisole: Evidence of Oxygen Removal in Reactions with Hydrogen. *Catal. Letters* **2011**, *141*, 817–820.

(23) Zhu, X.; Lobban, L. L.; Mallinson, R. G.; Resasco, D. E. Bifunctional Transalkylation and Hydrodeoxygenation of Anisole over a Pt/HBeta Catalyst. *J. Catal.* **2011**, *281*, 21–29.

(24) Zhu, X.; Nie, L.; Lobban, L. L.; Mallinson, R. G.; Resasco, D. E. Efficient Conversion of M -Cresol to Aromatics on a Bifunctional Pt/HBeta Catalyst. *Energy & Fuels* **2014**, *28*, 4104–4111.

(25) Gao, D.; Xiao, Y.; Varma, A. Guaiacol Hydrodeoxygenation over Platinum Catalyst: Reaction Pathways and Kinetics. *Ind. Eng. Chem. Res.* **2015**, *54*, 10638–10644.

(26) Lee, K.; Gu, G. H.; Mullen, C. A.; Boateng, A. A.; Vlachos, D. G. Guaiacol Hydrodeoxygenation Mechanism on Pt(111): Insights from Density Functional Theory and Linear Free Energy Relations. *ChemSusChem* **2015**, *8*, 315–322.

(27) Lu, J.; Behtash, S.; Mamun, O.; Heyden, A. Theoretical Investigation of the Reaction Mechanism of the Guaiacol Hydrogenation over a Pt(111) Catalyst. *ACS Catal.* **2015**, *5*, 2423–2435.

(28) Lu, J.; Wang, M.; Zhang, X.; Heyden, A.; Wang, F. B-O-4 Bond Cleavage Mechanism for Lignin Model Compounds over Pd Catalysts Identified by Combination of First-Principles Calculations and Experiments. *ACS Catal.* **2016**, *6*, 5589–5598.

(29) Shi, D.; Arroyo-Ramírez, L.; Vohs, J. M. The Use of Bimetallics to Control the Selectivity for the Upgrading of Lignin-Derived Oxygenates: Reaction of Anisole on Pt and PtZn Catalysts. *J. Catal.* **2016**, *340*, 219–226.

(30) Ferrin, P.; Simonetti, D.; Kandoi, S.; Kunkes, E.; Dumesic, J. a.; Nørskov, J. K.; Mavrikakis, M. Modeling Ethanol Decomposition on Transition Metals: A Combined Application of Scaling and Brønsted−Evans−Polanyi Relations. *J. Am. Chem. Soc.* **2009**, *131*, 5809–5815.

(31) Liu, B.; Greeley, J. Decomposition Pathways of Glycerol via C–H, O–H, and C–C Bond Scission on Pt(111): A Density Functional Theory Study. *J. Phys. Chem. C* **2011**, *115*, 19702–19709.

(32) Norton, P. R.; Davies, J. A.; Jackman, T. E. Absolute Coverages of CO and O on Pt(111); Comparison of Saturation CO Coverages on Pt(100), (110) and (111) Surfaces. *Surf. Sci.* **1982**, *122*, 593–600.

(33) Kresse, G.; Hafner, J. Ab Initio Molecular Dynamics for Liquid Metals. *Phys. Rev. B* **1993**, *47*, 558–561.

(34) Kresse, G.; Furthmüller, J. Efficiency of Ab-Initio Total Energy Calculations for Metals and Semiconductors Using a Plane-Wave Basis Set. *Comput. Mater. Sci.* **1996**, *6*, 15–50.

(35) Kresse, G.; Furthmüller, J. Efficient Iterative Schemes for Ab Initio Total-Energy Calculations Using a Plane-Wave Basis Set. *Phys. Rev. B* **1996**, *54*, 11169–11186.

(36) Dion, M.; Rydberg, H.; Schröder, E.; Langreth, D. C.; Lundqvist, B. I. Van Der Waals Density Functional for General Geometries. *Phys. Rev. Lett.* **2004**, *92*, 246401.

(37) Klimeš, J.; Bowler, D. R.; Michaelides, A. Chemical Accuracy for the van Der Waals Density Functional. *J. Phys. Condens. Matter* **2010**, *22*, 022201.

(38) Yildirim, H.; Greber, T.; Kara, A. Trends in Adsorption Characteristics of Benzene on Transition Metal Surfaces: Role of Surface Chemistry and van Der Waals Interactions. *J. Phys. Chem. C* **2013**, *117*, 20572–20583.

(39) Gautier, S.; Steinmann, S. N.; Michel, C.; Fleurat-Lessard, P.; Sautet, P. Molecular Adsorption at Pt(111). How Accurate Are DFT Functionals? *Phys. Chem. Chem. Phys.* **2015**, *17*, 28921–28930.

(40) Kresse, G.; Joubert, D. From Ultrasoft Pseudopotentials to the Projector Augmented-Wave Method. *Phys. Rev. B* **1999**, *59*, 1758–1775.

(41) Monkhorst, H. J.; Pack, J. D. Special Points for Brillouin-Zone Integrations. *Phys. Rev. B* **1976**, *13*, 5188–5192.

(42) Fleurat-Lessard, P.; Dayal, P. http://perso.ens-lyon.fr/paul.fleurat-lessard/ReactionPath.html.

(43) Henkelman, G.; Uberuaga, B. P.; Jónsson, H. A Climbing Image Nudged Elastic Band Method for Finding Saddle Points and Minimum Energy Paths. *J. Chem. Phys.* **2000**, *113*, 9901.

(44) Sheppard, D.; Terrell, R.; Henkelman, G. Optimization Methods for Finding Minimum Energy Paths. *J. Chem. Phys.* **2008**, *128*, 134106.

(45) Henkelman, G.; Jónsson, H. A Dimer Method for Finding Saddle Points on High Dimensional Potential Surfaces Using Only First Derivatives. *J. Chem. Phys.* **1999**, *111*, 7010.

(46) Heyden, A.; Bell, A. T.; Keil, F. J. Efficient Methods for Finding Transition States in Chemical Reactions: Comparison of Improved Dimer Method and Partitioned Rational Function Optimization Method. *J. Chem. Phys.* **2005**, *123*, 224101.

(47) Kästner, J.; Sherwood, P. Superlinearly Converging Dimer Method for Transition State Search. *J. Chem. Phys.* **2008**, *128*, 014106.

(48) Ihm, H.; Ajo, H. M.; Gottfried, J. M.; Bera, P.; Campbell, C. T. Calorimetric Measurement of the Heat of Adsorption of Benzene on Pt(111). *J. Phys. Chem. B* **2004**, *108*, 14627–14633.

(49) Campbell, J. M.; Seimanides, S.; Campbell, C. T. Probing Ensemble Effects in Surface Reactions. 2. Benzene Adsorption on Clean and Bismuth-Covered platinum(111). *J. Phys. Chem. B* **1989**, *92*, 815.

(50) Christmann, K.; Ertl, G.; Pignet, T. Adsorption of Hydrogen on a Pt(111) Surface. *Surf. Sci.* **1976**, *54*, 365–392.

(51) Lu, K. E.; Rye, R. R. Flash Desorption and Equilibration of H2 and D2 on Single Crystal Surfaces of Platinum. *Surf. Sci.* **1974**, *45*, 677–695.

(52) Steininger, H.; Lehwald, S.; Ibach, H. On the Adsorption of CO on Pt(111). *Surf. Sci.* **1982**, *123*, 264–282.

(53) Redhead, P. a. Thermal Desorption of Gases. *Vacuum* **1962**, *12*, 203–211.

(54) Campbell, C. T.; Sellers, J. R. V. Correction to "The Entropies of Adsorbed Molecules." *J. Am. Chem. Soc.* **2013**, *135*, 13998–13998.

(55) Campbell, C. T.; Sellers, J. R. V. The Entropies of Adsorbed Molecules. *J. Am. Chem. Soc.* **2012**, *134*, 18109–18115.

(56) Campbell, C. T.; Árnadóttir, L.; Sellers, J. R. V. Kinetic Prefactors of Reactions on Solid Surfaces. *Zeitschrift für Phys. Chemie* **2013**, *227*, 1–20.

(57) Chase, Jr., M. W.; Davies, C. A.; Downey, Jr., J. R.; Frurip, D. J.; McDonald, R. A.; Syverud, A. N. *NIST JANAF Thermodynamical Tables 1985*; National Institue of Standard and Technology, 1986.

(58) Stephenson, R. M.; Malanowski, S. *Handbook of the Thermodynamics of Organic Compounds*; Springer Netherlands, 1987.

(59) McEwen, J.-S.; Payne, S. H.; Kreuzer, H. J.; Kinne, M.; Denecke, R.; Steinrück, H.-P. Adsorption and Desorption of CO on Pt(111): A Comprehensive Analysis. *Surf. Sci.* **2003**, *545*, 47–69.

(60) Réocreux, R.; Huynh, M.; Michel, C.; Sautet, P. Controlling the Adsorption of Aromatic Compounds on Pt(111) with Oxygenate Substituents: From DFT to Simple Molecular Descriptors. *J. Phys. Chem. Lett.* **2016**, *7*, 2074–2079.

(61) Honkela, M. L.; Björk, J.; Persson, M. Computational Study of the Adsorption and Dissociation of Phenol on Pt and Rh Surfaces. *Phys. Chem. Chem. Phys.* **2012**, *14*, 5849–5854.

(62) Réocreux, R.; Huynh, M.; Michel, C.; Sautet, P. Controlling the Adsorption of Aromatic Compounds on Pt(111) with Oxygenate Substituents: From DFT to Simple Molecular Descriptors. *J. Phys. Chem. Lett.* **2016**, *7*, 2074–2079.

TOC Image

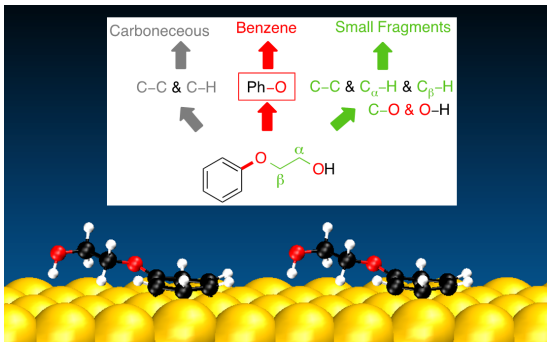
Carboneceous
Benzene
Small Fragments
C–C & C–H
Ph–O
C–C & Cα–H & Cβ–H
C–O & O–H
O
α
β
OH